Effects of lead and cadmium combined heavy metals on liver function and lipid metabolism in mice

Huaguo Chen (✉ chenhuaguo1981@163.com)
Guizhou Normal University

Chengxiang Zhu
Guizhou Normal University

Xin Zhou
Guizhou Normal University

Abstract

Although a large number of studies have been conducted on individual lead (Pb) or cadmium (Cd) exposures, the toxicity of combined Pb and Cd exposures is relatively limited. The present study aims to investigate toxicity of Pb-Cd combined heavy metals and its mechanism. A heavy metal exposure model was established by subcutaneous intragastric administration of Pb-Cd (50:1) for 35 days in mice. The body weight, diet, hair color, mental state, liver index, hematological index, biochemical indicators and pathological section were used to comprehensively evaluate the toxicity reaction. Then, classical oxidative stress indexes and lipidomics techniques had been used to explore the potential mechanism. The results showed that Pb-Cd could cause inappetite, poor spirit, significantly reduced activity, slow weight gain and dark hair color in mice. Pb-Cd could also cause liver enlargement, AST and ALT enzyme activities significantly increased, and pathological changes of liver. Prolonged exposure to c could also cause PCT, WBC, PLT and MON significantly increased, and RBC, HGB, HCT and LYM decreased. Pb-Cd can increase the oxidative stress by increasing the activity of SOD and LDH and the content of MDA. Pb-Cd also could cause lipid metabolism disorders by regulating linoleic acid metabolism, sphingolipid metabolism and glycerolipid metabolism.

1. Introduction

Heavy metals refer to metals with specific gravity greater than 4 or 5, with about 45 species, such as copper (Cu), lead (Pb), zinc (Zn), cadmium (Cd), mercury (Hg), and silver (Ag) (Chai et al. 2021). Although manganese, copper, Zn and other heavy metals are trace elements needed for life activities, most of them, such as Pb and Cd are not necessary, and all heavy metals above a certain concentration are toxic to the human body (Mansoor et al. 2021). For example, after Pb enters the human body, except part of it is excreted through feces and sweat, the rest is dissolved into the blood after several hours, hindering the synthesis of blood, leading to anemia, headache, dizziness, fatigue, sleepiness, constipation and limb soreness (Kan et al. 2021). Cd enters the human body and forms Cd-thionein, which reaches the whole body through the blood and is selectively stored in the kidney and liver (Samuel et al. 2021). Since heavy metals are extremely harmful to human body, scientists have carried out a lot of research work on the damage caused by heavy metals. Mengjiao Bi et al. (Bi et al. 2019) reported the molecular mechanisms of Pb-induced changes of selenium status in mice livers through interacting with selenoprotein P. The research results of Debashis Reja et al (Reja et al. 2020) showed that blood Pb level was associated with advanced liver fibrosis in patients with non-alcoholic fatty liver disease. Damir Suljevic et al. (Suljevic et al. 2019) thought that chronic Cd exposure in vivo could cause damage to bone marrow hematopoietic cells, followed by severe red blood cell damage and liver necrosis. Eunjung Park et al. (Park et al. 2021) conducted a study on the relationship between environmental Cd exposure and the risk of suspected non-alcoholic fatty liver disease.

In fact, although a large number of studies have been conducted with positive results on individual Pb or Cd exposures, the toxicity of combined Pb and Cd exposures is relatively limited. However, in some special environments, such as the mining of Pb and Zn mines, there is a large amount of heavy metal

pollution, and Pb and Cd are associated. The effects of combined exposure of Pb and Cd on human health are not clear. Therefore, mice were used as the research carrier in this study to focus on the damage of combined exposure of Pb and Cd on their liver, so as to provide a basis for toxicity evaluation of combined exposure of heavy metals.

2. Materials And Methods

2.1 Materials

Enzyme-linked immunosorbent assay (ELISA) Kits of alanine aminotransferase (ALT), aspartate aminotransferase (AST), superoxide dismutase (SOD), malondialdehyde (MDA), lactate dehydrogenase (LDH) and glutathione peroxidase (GSH-Px) were obtained from Shanghai Guduo Biotechnology Co., Ltd. Lead acetate ($Pb(CH_3COO)_2$) and cadmium chloride ($CdCl_2$) were obtained from Tianjin Komil Chemical Reagent Co., Ltd. All other reagents were analytical grade.

2.2 Animals

KM species SPF grade male mice (body weight 18–22 g) were purchased from Changsha Tianqin Biotechnology Co., Ltd. (License No. SCXK-2019-0014). They were bred in the Guizhou Engineering Laboratory for Quality Control & Evaluation Technology of Medicine with the relative temperature of 20°C – 25°C and humidity of 60% – 75%. All experiments on animal in this study was been conducted according to the Guide of the Care and Use of Laboratory Animal, Eighth Edition (Council 2010) and approved by the Guizhou Normal University Animal Care and Use Committee.

2.3 Modeling and group administration

3.66 and 0.08 grams of $Pb(CH_3COO)_2$ and $CdCl_2$ samples were accurately weighed in a 50 ml volumetric flask, and dissolved with pure water to the volume.

Twenty KM male mice were fed adaptive for 3 days and randomly divided into 2 groups with 10 mice in each group, which were blank control group and Pb-Cd group. The blank control group was intragastrically given normal saline twice a day at an interval of 2 h. Pb-Cd model model group was intragastrically administrated with Pb and Cd complex solution once a day, and then intragastrically administrated with normal saline once a day. The whole observation period was 5 weeks, and the intragastric dose was 0.01 ml per gram of mice.

2.4 Observation and recording of routine indexes

During modeling and administration, food and drinking water were provided as usual. The fur color, dietary status, urine and feces, and mental status of the mice were observed and recorded. Meanwhile, the mice were weighed every 3 days until the end of the fifth week of the experiment. After the last modeling and administration, the mice were fasted without water for 12 h, and the final body weight of the mice was recorded.

2.5 Collection of tissue samples

After the experiment lasted for 5 weeks, tissue samples were collected. Blood was collected from the ipsilateral orbit of the mice, and collected in a centrifuge tube with heparin sodium anticoagulant. The blood was shook back and forth to prevent blood coagulation, and then stored in a 4°C refrigerator for later use. The mice were sacrificed by cervical dislocation after blood collection and the liver was quickly dissected. The blood on the surface of the organs was washed in normal saline and drained with filter paper. The organs were weighed on an analytical balance to calculate the organ index.

$$\text{Liver index} = \frac{\text{liver weight}}{\text{body weight of mice}} \times 100\%$$

Then, small pieces of liver tissue from the same part were cut and fixed in 10% formaldehyde fixation solution and refrigerated at 4°C for pathological sections. The rest tissues were divided into two parts and stored in a -80°C refrigerator for the detection of biochemical indexes and lipid analysis, respectively.

2.6 Determination of blood indicators

Red blood cell (RBC), white blood cell (WBC), hemoglobin (HGB), platelet (PLT), thrombocyte hematocrit (PCT), hematocrit (HCT), lymphocyte (LYM) and monocyte (MON) in blood samples were detected and analyzed by a hematology analyzer.

2.7 Determination of AST and ALT activity

After the liver tissue was removed from the refrigerator and thawed to room temperature, 0.10 g was accurately weighed and placed in a 5 ml centrifuge tube, 0.9 mL of normal saline was added and homogenized in a homogenizer, then centrifuged at 4°C and 3000 $r.min^{-1}$ for 10 min. The supernatant was absorbed and placed in a low temperature (4°C) environment for later use. Finally, the activities of AST and ALT in liver tissue of mice in each group was measured according to the instructions of the kits.

2.8 Histopathological analysis

Liver samples fixed with 10% formaldehyde were embedded in paraffin and sectioned, stained with hematoxylin and eosin (HE), and sealed with neutral gum. The morphological changes of liver tissue in each group were observed under light microscope.

2.9 Determination of oxidative stress indicators

The administration of the animals and collection of liver samples were consistent with those described in Section 2.3 and Section 2.5. 0.1 gram of liver sample was accurately weighed into a 5 ml centrifuge tube and 0.9 ml of normal saline was added for homogenization. The mixture was centrifuged at 4°C and 3000 $r.min^{-1}$ for 10 min. The supernatant was taken to determine the activities of SOD, GSH-Px and LDH and the content of MDA according to the kits instruction.

2.10 Lipidomic analysis

2.10.1 Lipid extraction

The liver tissue samples of each group were thawed step by step, and 0.2 g of liver tissue was accurately weighed into a centrifuge tube, and 600 μL iced methanol (stored overnight at -20°C) and 150 μL pure water were added, respectively. After the mixture was homogenized in a homogenizer, 450 μL dichloromethane was added to swirl for 30 s at 3000 r, and then 150 μL pure water was added to swirl for 1 min. The swirled mixture was placed at room temperature for 5 min, then centrifuged at a high speed of 12000 r·min^{-1} at -6°C for 15 min. The lower liquid was taken into a 1.5 mL centrifuge tube and dried with nitrogen. Before detection and analysis, a mixture of 200 μL acetonitrile: isopropanol: water (65:30:5) was added and centrifuged at 4°C, 8000 r·min^{-1} for 5 min. The supernatant was collected through a 0.22 μm microporous filter membrane and placed in an injection flask for UHPLC-MS-MS analysis.

2.10.2 Quality control sample preparation

Liver tissue homogenates of each group were mixed in equal volume and treated as quality control (QC) samples according to the same method in Section 2.10.1, so as to evaluate the stability and repeatability of the system.

2.10.3 Chromatographic separation conditions

The samples were separated using the DiONEX™ Ultimate™ 3000 ultra performance liquid chromatography system and connected to an ACE Excel 1.7C$_{18}$-AR (2.1×100 mm, 1.7 μm) column. The mobile phase consisted of A (0.1% acetic acid water) and B (acetonitrile, containing 0.1% acetic acid), and the elution conditions were as follows: from 0 to 2 min, the proportions of A and B maintained at 50%; from 2 to 25 min, mobile phase A decreased from 50–10%, and mobile phase B increased from 50–90%; from 25 to 30 min, mobile phase A returned from 10–50%, and mobile phase B decreased from 90–50%. The flow rate, injection volume and column temperature were set at 300 μL m-1, 4 μL and 40°C, respectively.

2.10.4 Mass spectrometric analysis conditions

The positive and negative ion modes of the samples were detected by Q Exactivetm mass spectrometry. The ion source was HESI, and the parameters of the ion source were as follows: Set the SPray Voltage to 3.5 kV (+) /3.2 kV (-), CaPillary Temperature to 320°C, Probe heating Temperature to 350°C, and the Sweep Gas to 0 arb. Sheath Gas and AUX Gas were 35 arb and 10 arb, respectively. The full scan of primary mass spectrometry was 100–1000 mass charge ratio, and the mass resolution was 70000.

2.10.5 Non-targeted lipidomic data processing

Progenesis QI software was used to perform peak alignment and peak extraction on the original mass spectrum to obtain lipid data. After standardized pretreatment, lipid mass spectrum data of retention time (RT), mass to charge ratio (m/z) and peak intensity were obtained. For the obtained lipid mass spectrum

data, the lipid data with a deletion value of more than 50% in the group and the lipid data with a RSD of more than 30% in the quality control samples were deleted, and then the total peak area was normalized. SIMCA 14.1 software was used for pattern recognition of the mass spectrum data. After preprocessing by UV and Pareto-scaling modes, unsupervised principal component analysis (PCA) and orthogonal partial least multiplicative discriminant analysis (OPLS-DA) were performed. Then, SPSS 21.0 and Metaboanalyst 5.0 were used for t-test, multiple of variation and other one- dimensional statistical analysis.

3. Results And Discussion

3.1 Routine index analysis

When the body is damaged by heavy metals such as Pb or Cd, the body weight, diet, hair color and mental state will also change (Dai et al. 2021). Therefore, the poisoning situation of the body and the intervention situation of therapeutic substances can be judged to a certain extent through the observation of conventional indicators. In this study, there were no significant differences in body weight, diet, hair color and mental state during adaptive feeding. During the experiment period of 5 weeks, mice in the blank control group had flexible response, good appetite and bright fur. Compared with the blank control group, mice in the Pb-Cd model group showed inappetite, poor spirit, significantly reduced activity, slow weight gain and dark hair color (Fig. 1). The results showed that combined exposure to Pb and Cd caused damage to body weight, mental state and hair in mice.

In addition, when the body is damaged by Pb and Cd complex heavy metals, a series of changes will occur in cell morphology, substance metabolism and so on, leading to changes in organ index. Therefore, the analysis of organ index can reflect the liver injury of mice. In this study, the liver index of each group was measured. As can be seen from Table 1, the liver index of Pb and Cd model group was $4.15 \pm 0.33\%$, which was significantly higher than that of blank control group ($P < 0.01$), the results showed that combined exposure to Pb and Cd could cause liver enlargement in mice.

Table 1
Changes of liver indexes in mice of each
group. ($\bar{x} \pm$ SD, n = 10)

Group	Liver index (%)
Blank control group	3.51 ± 0.19
Pb-Cd group	4.15 ± 0.33**
Note: * Compared with blank control group, **P<0.01.	

3.2 Hematological index analysis

Long-term exposure to Pb or Cd pollution will lead to damage to blood quality, therefore, hematological indicators are often used to evaluate the degree of harm of heavy metals to the body and the efficacy of therapeutic agents (Rehman et al. 2021). In the present study, hematological index of RBC, WBC, HGB, PLT, PCT, HCT, LYM and MON were monitored. As shown in Table 2, compared with the blank group, PCT in the Pb-Cd group was significantly increased (P < 0.05), WBC, PLT and MON showed an upward trend, while RBC, HGB, HCT and LYM showed a downward trend.

Table 2
Changes of blood index and Biochemical index in
mice. ($\bar{x}$ ± SD, n = 10)

Group	Blank control group	Pb-Cd group
WBC	5.71 ± 1.72	6.35 ± 0.36
RBC	7.31 ± 0.27	7.07 ± 0.35
HGB	151.56 ± 4.38	149.24 ± 8.18
PLT	222.60 ± 28.42	330.90 ± 47.61[*]
PCT	0.25 ± 0.04	0.47 ± 0.15[**]
HCT	37.33 ± 0.96	36.77 ± 2.12
LYM	2.86 ± 0.51	1.99 ± 0.25
MON	1.24 ± 0.26	2.01 ± 0.14[*]
AST(U/L)	33.25 ± 1.46	38.25 ± 3.89[**]
ALT(U/L)	54.20 ± 4.69	60.72 ± 4.62[**]

Note: * Compared with blank control group, *P<0.05; **P<0.01.

3.3 ALT and AST analysis

Liver function examination is the examination item that reflects liver physiology function (Ragab AboZaid et al. 2021). There are many liver function indicators, including ALT, AST, total bilirubin, direct bilirubin, indirect bilirubin, alkaline phosphatase, glutamyl transpeptidase, albumin, globulin, prealbumin, total bile acid, etc. These indicators can reflect whether there is damage to liver cells, whether there is obstruction of the biliary tract, but also reflect the synthetic function of the liver (Zubrzycki et al. 2020). For example, in humans, the normal value of AST is 8–40 U/L, and when ALT is significantly elevated and the AST/ALT ratio is greater than 1, damage to liver parenchyma is indicated. In the present study, ALT and AST indexes of different groups of mice were systematically observed, and the results were shown in Table 2.

Compared with the blank control group, the AST and ALT enzyme activities in the Pb-Cd group were significantly increased (P < 0.01), indicating that Pb and Cd complex heavy metals did have significant damage to the liver.

3.4 Pathological analysis

In order to explore the disease process of organs, tissues or cells, some pathomorphological examination method can be used to examine their lesions, discuss the causes, pathogenesis and development process of lesions, and finally make pathological diagnosis (Murakami et al. 2020). Pathological examination has been widely used in clinical work and scientific research (Baraban et al. 2020). In this study, in order to explore the liver injury of mice exposed to Pb and Cd, HE staining was performed to evaluate the histopathological changes of mouse liver.

The prepared sections were observed under a microscope, and the results were shown in Fig. 2. The liver tissue structure of mice in the blank control group was complete, with clear morphology, orderly arrangement of liver cells, normal structure and distinct hierarchy. The liver cells of Pb-Cd group were massive necrosis, uneven arrangement, vacuolar degeneration and congestion.

3.5 Analysis of the oxidative stress index

There are many studies on the toxicological mechanism of heavy metals on body damage (Wallace and Buha Djordjevic 2020). Studies have shown that long-term exposure to lead or cadmium can cause oxidative stress damage to the body (Briffa et al. 2020). In this study, classical oxidative stress targets such as SOD, GSH-Px, MDA and LDH were used to evaluate the toxicology mechanism of Pb-Cd induced liver injury in mice.The results were shown in Table 3. Compared with the blank group, the activities of SOD and LDH in Pb-Cd group were significantly increased (P < 0.01), while the content of MDA was significantly increased (P < 0.01), and the activity of GSH-Px was decreased. These results indicated that Pb-Cd could indeed cause the disorder of oxidative stress indexes in the body, thus damaging the health of the body.

Table 3
Changes of SOD, GSH-PX, LDH activities and MDA content
in liver tissues of mice in each group,$\bar{x} \pm SD$ (n = 10)

Group	Blank control group	Pb-Cd group
SOD(U/ml)	146.62 ± 4.14	180.83 ± 7.57[**]
GSH-PX(U/L)	442.42 ± 23.81	421.82 ± 36.15
MDA(nmol/ml)	3.60 ± 0.21	4.20 ± 0.28[**]
LDH(IU/L)	4.53 ± 0.21	5.17 ± 0.16[**]
Note: * Compared with blank control group, **P<0.01.		

3.6 Analysis of lipidomics

In recent years, omics technology has been developed vigorously with the development of analytical chemistry technology (Marvasi et al. 2019). Metabolomics is a discipline that reflects the endogenous and exogenous changes of the body and provides further understanding of the disease (Feizi et al. 2021). Lipidomics is an important branch of metabolomics. The changes of lipid metabolism under different physiological and pathological conditions are analyzed and compared to reflect the changes of physiology and pathology (Wu et al. 2021). Therefore, in addition to studying the toxic mechanism of lead and cadmium from the perspective of classical oxidation targets, this study also used non-targeted lipidomics to analyze the changes in liver tissue of mice in each group and to search for possible lipid regulatory pathways.

3.6.1 Quality control of non-targeted lipidomics data

In the process of this study, 5 QC samples were randomly inserted during the detection of liver samples from each group of mice to verify the reliability of the experimental method and the stability of the instrument. Unsupervised PCA analysis was conducted on the pre-processed QC sample data of the five samples, and the results were shown in Fig. 3.

The results showed that the QC samples were all within 2std, indicating that the experimental method was reliable and the instrument had good stability.

3.6.2 Multivariate statistical analysis of lipid data

After the pre-treatment of the original lipid data of each group, Metaboanalyst 5.0 (https://www.metaboanalyst.ca/) was used for data processing such as missing value and normalization of total peak area, and SIMCA 14.1 software was used for multivariate statistical analysis of the processed data.

Firstly, PCA statistical analysis was performed on the lipid data of liver tissue of mice in each group to obtain PCA score under positive and negative ion mode. As can be seen from Fig. 4, the lipid data of liver tissue in the blank group and the Pb-Cd group were well separated. The results showed that the two groups of mice could be distinguished normally, suggesting that Pb-Cd had a significant effect on lipid disorders.

In order to further screen out the different lipids, the mass spectrometry data of the blank control group and Pb-Cd model group were further analyzed by supervised OPLS-DA. As shown in Fig. 5A and 5B, parameter R^2x of the OPLS-DA model represented the fitting degree of the model, and parameter Q^2 represented the prediction ability of the model. In **Fig. 5A**, $R^2X = 0.564$ (cum) and $Q^2 = 0.9$ (cum) in the blank control group and Pb-Cd group in the negative ion mode, where R^2 was greater than 0.5, the difference between R^2X and Q^2 was less than 4, and Q^2 was close to 1, indicating that it had good fitting

and prediction ability in the negative ion mode. Similarly, as shown in Fig. 5B, in the positive ion mode, $R^2X = 0.515$ (cum), $Q^2 = 0.88$ (cum), $R^2 > 0.5$, the difference between R^2X and Q^2 was less than 3, and Q^2 was close to 1, indicating that lipids in liver tissues had good fitting and prediction ability in the positive ion mode. In order to prevent over-fitting of the OPLS-DA model, 200 displacement tests were carried out for the establishment of the OPLS-DA model, as shown in Fig. 5C and 5D. Both the y-intercepts of Q^2 in positive and negative ion modes were less than 0, indicating that no over-fitting occurred in the OPLS-DA model and the results were reliable.

Volcano map is a combination of multiple of variation analysis and T test, which can intuitively show the significance of lipid changes between the two groups of samples. Through experimental screening of the FC values in the blank group and Pb-Cd group, a volcano diagram was made for the screened differential lipids, as shown in Fig. 6, Log2 (FC) was the abscissa and -Log10 (P) was the ordinate.

As can be seen from the Fig. 6, there were obvious differences in lipids between the blank group and Pb-Cd group, in which the blue color indicated down-regulation, and the red color indicated up-regulation, indicating that the lipid metabolites in the liver tissues of mice had undergone great changes after the lead and cadmium complex heavy metals were poisoned.

3.6.3 Screening of differential lipids

In order to further screen differential lipids, VIP > 1, P < 0.05, FC > 2 or FC < 0.5 were used as parameters for screening differential metabolites. According to LIPID MAPS, HMDB, Massbank of North America (MONA) and other online sites, the LIPID ratio and secondary mass spectrometry were compared. A total of 24 different lipids were identified, and the specific substances were shown in Table 4.

Table 4
Differential lipid table of Blank group and Pb-Cd group.

Compound name	Formula	Class	RT	m/z	VIP	FC	P-value
Stearoyl-L-Carnitine	C25H49NO4	FA	6.56	426.342	1.022	8.800	0.016
Pentaethylene glycol	C23H45NO4	FA	5.96	426.342	1.307	7.872	0.017
6-Aminohexanoate	C6H13NO2	FA	15.62	392.316	1.504	2.633	0.002
Linoleic acid	C18H32O2	FA	11.60	456.332	1.210	3.703	0.003
LPE 20:5	C25H42NO7P	GP	5.64	500.276	4.172	0.443	0.002
PE (18:1/22:6)	C45H76NO8P	GP	23.69	790.536	1.014	0.387	0.004
LPE 18:0	C23H48NO7P	GP	9.87	480.308	7.000	0.484	0.005
PC(P-18:1/P-18:1)	C44H86NO7P	GP	21.01	340.356	1.373	2.310	0.006
PC(16:0/18:1)	C42H82NO8P	GP	19.78	703.468	1.130	6.477	0.045
LPE(20:3)	C25H46NO7P	GP	11.56	580.361	1.538	0.394	0.000
PG(22:6/18:0)	C46H79O10P	GP	23.76	738.507	1.795	0.487	0.020
PC(16:0/20:5)	C44H78NO8P	GP	24.40	764.548	2.263	2.889	0.025
LPE(18:2)	C23H44NO7P	GP	23.17	712.491	1.027	0.478	0.042
LPE 14:1	C19H38NO7P	GP	13.06	342.336	5.239	3.660	0.000
LPE 16:1	C21H42NO7P	GP	15.93	370.367	2.846	2.170	0.001
PE (16:0/20:5)	C41H72NO8P	GP	23.36	738.505	5.256	0.314	0.001
PE (20:5/22:6)	C47H72NO8P	GP	20.67	808.491	1.677	0.450	0.001
Bexarotene	C24H28O2	PR	23.45	762.507	4.048	0.371	0.000
agnuside	C22H26O11	PR	19.75	465.304	5.365	0.416	0.000
Ginkgolide B	C20H24O10	PR	17.86	572.480	3.202	2.321	0.000
Abietic acid	C20H30O2	PR	5.62	498.262	4.345	0.426	0.001
SM(d18:1/18:0)	C41H83N2O6P	SP	9.09	762.556	1.362	17.399	0.014
SM(d18:0/16:0)	C39H81N2O6P	SP	22.04	618.476	1.006	0.498	0.003
Sphingosine-1-Phosphate	C18H38NO5P	SP	11.57	366.336	4.498	2.834	0.002

Cluster analysis was performed on the 24 different lipid metabolites screened, which could more comprehensively and intuitively display the relationship between the samples and the expression patterns

of different groups of lipids. As shown in Fig. 7, there were significant differences in metabolites between the Pb-Cd group and the blank group. The experimental results showed that Pb-Cd complex heavy metals could cause a significant lipid metabolism disorder.

3.4.4 Pathway analysis and biological interpretation

Among the 24 differential lipid metabolites screened, 12 differential lipids were down-regulated in the Pb-Cd model group compared with the blank control group, including PC (P-18:1/P-18:1), PC (16:0–18:1), SM (d18:1/18:0), Ginkgolide B, PC (16:0/20:5), Stearoyl-L-Carnitine, Pentaethylene glycol, Aminocaproic acid, LPE (16:1), LPE (14:1), Sphingosine-1-Phosphate and Linoleic acid. While PG (22:6/18:0), LPE (18:2), LPE (18:0), agnuside, PE (20:5/22:6), PE (18:1/22:6), PE (16:0/20:5), Bexarotene, SM (d18:0–16:0), LPE (20:3), LPE (20:5) and Abietic acid were up-regulated. The 24 selected differential lipids included four major categories of fatty acyl, glycerol phospholipids, enol esters and sphingolipids, and 11 subcategories of fatty acid esters, fatty acid conjugates, linear acid derivatives, glycerol phospholipid ethanolamine, glycerol phospholipid choline, glycerol phosphate glyceride, vitamin A-like, terpene glycoside, terpene lactone, diterpene and sphingolipids. According to the HMDB ID number of differential lipids, the pathways of 24 differential lipids were analyzed using Metaboanalyst 5.0 online site.

The results were shown in Fig. 8, where the color red represented a low P value, and the circle size represented the path influence value, and the larger the influence value is, the higher the influence value is. A total of 8 pathways were identified, including Linoleic acid metabolism, sphingolipid metabolism, Glycerophospholipid metabolism, alpha-Linolenic acid metabolism, arachidonic acid metabolism, glycosylphosphatidylinositol-anchor biosynthesis, biosynthesis of unsaturated fatty acids and fatty acid degradation. Among them, linoleic acid metabolism was the most influential pathway, followed by sphingolipid metabolism and glycerol phospholipid metabolism. The results showed that Pb-Cd could cause lipid disorders, possibly by regulating linoleic acid metabolism, sphingolipid metabolism and glycerolipid metabolism.

4. Conclusion

In this study, combined exposure of Pb and Cd to mice was evaluated. Long-term exposure to Pb and Cd resulted in loss of appetite, poor mental performance, significantly reduced activity, slow weight gain, and dark hair color in mice. It can also lead to liver enlargement, liver tissue and cell changes, and elevated ALT and AST. Pb-Cd could indeed cause the disorder of oxidative stress indexes in the body, thus damaging the health of the body. The combined exposure of Pb and Cd can also lead to the disorder of lipid metabolism in the body and induce a variety of diseases.

Abbreviations

ALT, alanine aminotransferase, AST, aspartate aminotransferase, SOD, superoxide dismutase, MDA, malondialdehyde, LDH, lactate dehydrogenase, GSH-Px, glutathione peroxidase, RBC, red blood cell, WBC, white blood cell, HGB, hemoglobin, PLT, platelet, PCT, thrombocyte hematocrit, HCT, hematocrit, LYM,

lymphocyte, MON, monocyte, QC, quality control, PCA, principal component analysis, OPLS-DA, orthogonal partial least multiplicative discriminant analysis.

Declarations

Funding

Competing Interests

The authors declare they have no financial interests.

Author Contributions

All authors contributed to the study conception and design. Material preparation, data collection and analysis were performed by [Huaguo Chen], [Chengxiang Zhu] and [Xin Zhou]. The first draft of the manuscript was written by [Huaguo Chen] and all authors commented on previous versions of the manuscript. All authors read and approved the final manuscript.

Data Availability

The datasets generated during and/or analysed during the current study are available from the corresponding author on reasonable request.

Supporting information

The representative total ion current (TIC) spectra of rats in the blank group, QC sample and Pb-Cd group samples are provided in the Supporting Information.These materials are available free of charge on the Internet at https://www. springer. com/journal.

References

1. Baraban, E., Tong, C.C.L., Adappa, N.D. and Cooper, K. 2020. A subset of sinonasal undifferentiated carcinoma is associated with transcriptionally active high-risk human papillomavirus by in situ hybridization: a clinical and pathologic analysis. Human Pathology 101, 64–69. https://doi.org/10.1016/j.humpath.2020.05.002

2. Bi, M., Zhang, H., Yuan, L., Zhao, L. and Liu, R. 2019. Molecular mechanisms of lead-induced changes of selenium status in mice livers through interacting with selenoprotein P. Ecotoxicology and Environmental Safety 175, 282–288. https: //doi.org/10.1016/j.ecoenv.2019.03.059

3. Briffa, J., Sinagra, E. and Blundell, R. 2020. Heavy metal pollution in the environment and their toxicological effects on humans. Heliyon 6, e04691. https://doi.org/10.1016/j.heliyon.2020.e04691

4. Chai, W.S., Cheun, J.Y., Kumar, P.S., Mubashir, M., Majeed, Z., Banat, F., Ho, S.-H. and Show, P.L. 2021. A review on conventional and novel materials towards heavy metal adsorption in wastewater treatment application. Journal of Cleaner Production 296, 126589. https://doi.org/10.1016/j.jclepro.2021.126589

5. Council, N. 2010. Guide for the Care and Use of Laboratory Animals: Eighth Edition. Publication 327, 963–965. https://doi.org/10.17226/12910

6. Dai, S., Chen, Q., Jiang, M., Wang, B., Xie, Z., Yu, N., Zhou, Y., Li, S., Wang, L., Hua, Y. and Tian, B. 2021. Colonized extremophile Deinococcus radiodurans alleviates toxicity of cadmium and lead by suppressing heavy metal accumulation and improving antioxidant system in rice. Environmental Pollution 284, 117127. https://doi.org/10.1016/j.envpol.2021.117127

7. Feizi, N., Hashemi-Nasab, F.S., Golpelichi, F., Saburouh, N. and Parastar, H. 2021. Recent trends in application of chemometric methods for GC-MS and GC×GC-MS-based metabolomic studies. TrAC Trends in Analytical Chemistry 138, 116239. https://doi.org/10.1016/j.trac.2021.116239

8. Kan, X., Dong, Y., Feng, L., Zhou, M. and Hou, H. 2021. Contamination and health risk assessment of heavy metals in China's lead–zinc mine tailings: A meta–analysis. Chemosphere 267, 128909. https://doi.org/10.1016/j.chemos phere.2020.128909

9. Mansoor, S., Kour, N., Manhas, S., Zahid, S., Wani, O.A., Sharma, V., Wijaya, L., Alyemeni, M.N., Alsahli, A.A., El-Serehy, H.A., Paray, B.A. and Ahmad, P. 2021. Biochar as a tool for effective management of drought and heavy metal toxicity. Chemosphere 271, 129458. https://doi.org/10.1016/j.chemosphere.2020.129458

10. Marvasi, M., Cavalieri, D., Mastromei, G., Casaccia, A. and Perito, B. 2019. Omics technologies for an in-depth investigation of biodeterioration of cultural heritage. International Biodeterioration & Biodegradation 144, 104736. https://doi.org/ 10.1016/j.ibiod.2019.104736

11. Murakami, I., Ohno, A., Ikeda, M., Yamashita, H., Mikami, M., Kobayashi, Y., Nagase, S., Yokoyama, M., Enomoto, T. and Katabuchi, H. 2020. Analysis of pathological and clinical characteristics of cervical conization according to age group in Japan. Heliyon 6, e05193. https://doi.org/10.1016/j.heliyon.2020.e05193

12. Park, E., Kim, J., Kim, B. and Park, E.Y. 2021. Association between environmental exposure to cadmium and risk of suspected non-alcoholic fatty liver disease. Chemosphere 266, 128947. https://doi.org/10.1016/j.chemosphere.2020.128947

13. Ragab AboZaid, O.A., Mahfouz, M.K., Abdel hammed, O.M., Maksoud H.A, A., Elwan, A.W., Abdallah, O.E. and Elharrif, M.G. 2021. Sofosbuvir plus ribavirin combination regimen boost liver functions and antioxidant profile in hepatitis C virus patients. Microbial Pathogenesis 150, 104740. https://doi.org/10.1016/j. micpath.2021.104740

14. Rehman, A.U., Nazir, S., Irshad, R., Tahir, K., ur Rehman, K., Islam, R.U. and Wahab, Z. 2021. Toxicity of heavy metals in plants and animals and their uptake by magnetic iron oxide nanoparticles. Journal of Molecular Liquids 321, 114455. https://doi.org/10.1016/j.molliq.2020.114455

15. Reja, D., Makar, M., Visaria, A., Karanfilian, B. and Rustgi, V. 2020. Blood lead level is associated with advanced liver fibrosis in patients with non-alcoholic fatty liver disease: A nationwide survey (NHANES 2011–2016). Annals of Hepatology 19, 404–410. https://doi.org/10.1016/j.aohep.2020.03.006

16. Samuel, M.S., Datta, S., Khandge, R.S. and Selvarajan, E. 2021. A state of the art review on characterization of heavy metal binding metallothioneins proteins and their widespread applications. Science of The Total Environment 775, 145829. https://doi.org/10.1016/j.scitotenv.2021.145829

17. Suljevic, D., Corbic, A., Islamagic, E., Focak, M., Filipic, F. and Alijagic, A. 2019. Impairments of bone marrow hematopoietic cells followed by the sever erythrocyte damage and necrotic liver as the outcome of chronic in vivo exposure to cadmium: novel insights from quails. Environmental Toxicology and Pharmacology 72, 103250. https://doi.org/10.1016/j.etap.2019.103250

18. Wallace, D.R. and Buha Djordjevic, A. 2020. Heavy metal and pesticide exposure: A mixture of potential toxicity and carcinogenicity. Current Opinion in Toxicology 19, 72–79. https://doi.org/10.1016/j.cotox.2020.01.001

19. Wu, B., Wei, F., Xu, S., Xie, Y., Lv, X., Chen, H. and Huang, F. 2021. Mass spectrometry-based lipidomics as a powerful platform in foodomics research. Trends in Food Science & Technology 107, 358–376. https://doi.org/10.1016/j. tifs.2020.10.045

20. Zubrzycki, A., Wrońska, A., Kotulak-Chrząszcz, A., Wierzbicki, P.M. and Kmieć, Z. 2020. Fenofibrate impairs liver function and structure more pronounced in old than young rats. Archives of Gerontology and Geriatrics 91, 104244. https://doi.org/10.1016/j.archger.2020.104244
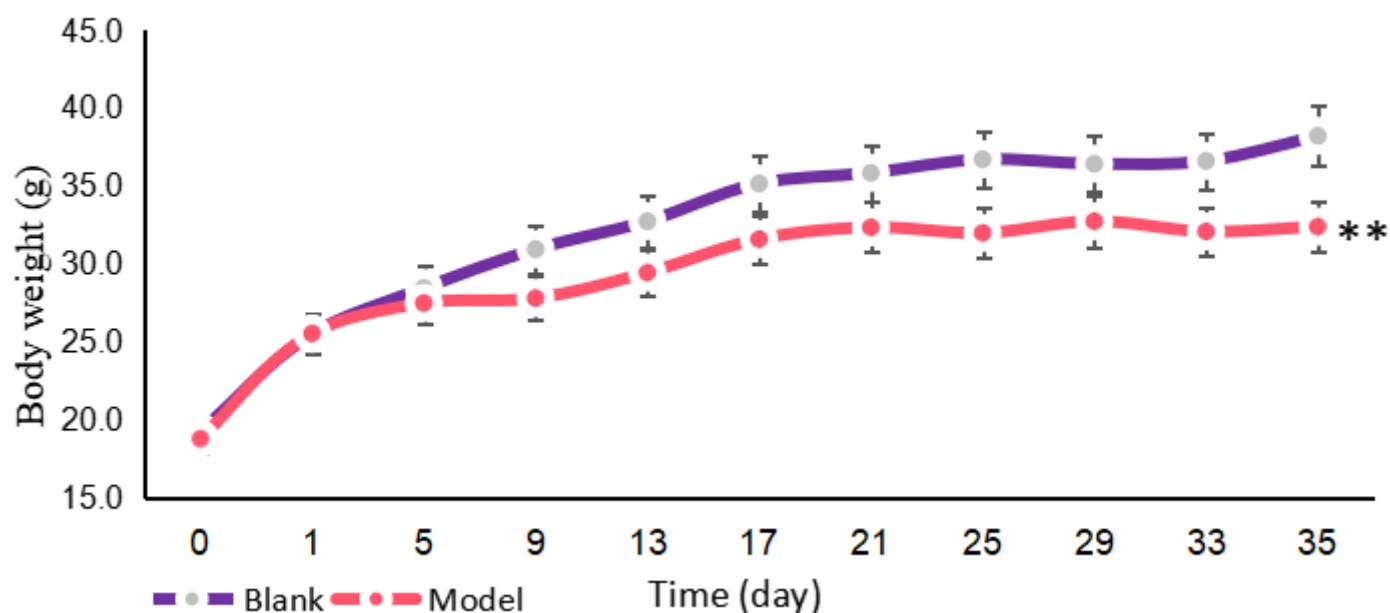
Figures

Figure 1

Changes of body weight in mice.

Note: * Compared with blank control group, **$P<0.01$.

Figure 2

Each group of mice liver tissue pathological section (400X). A: Blank control group; B: Pb-Cd group.
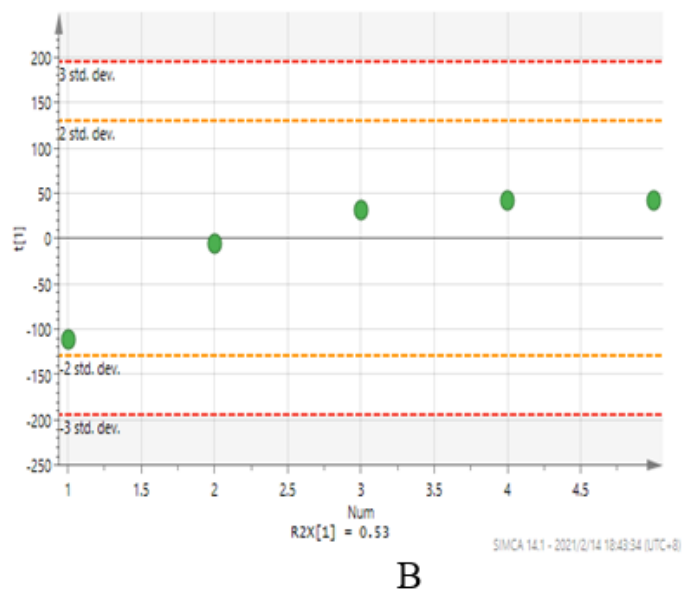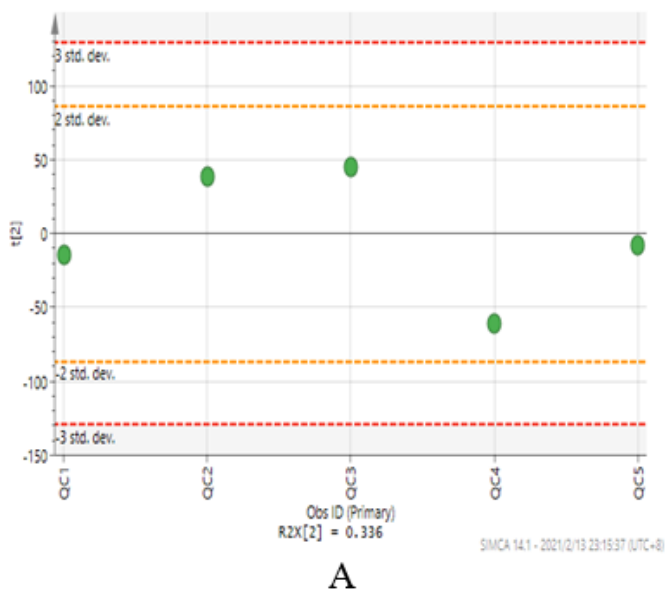

A

B

Figure 3

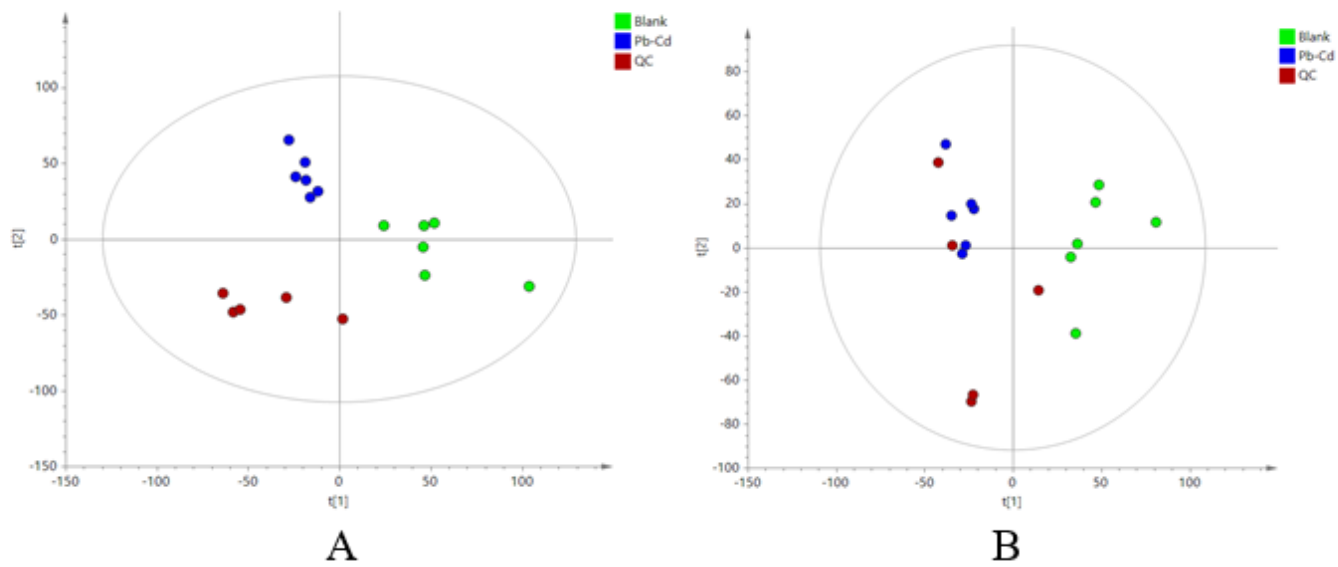PCA score chart of QC sample (A: Negative ion mode; B: Positive ion mode).

Figure 4

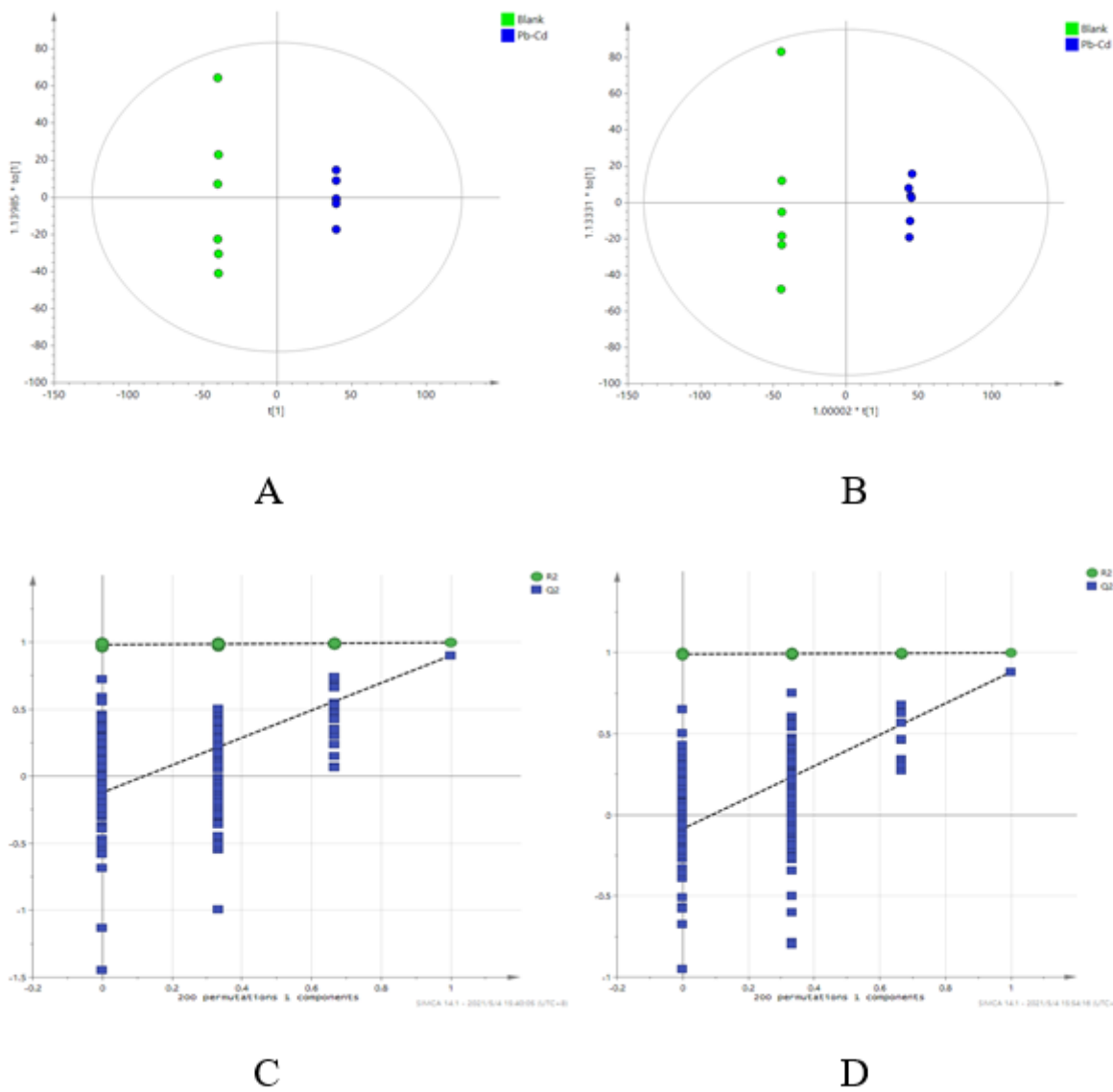PCA score of each group (A: Negative ion mode; B: Positive ion mode).

Figure 5

OPLS-DA score map and OPLS-DA model response permutation verification map between blank control group and Pb-Cd group(A, C: Negative ion mode; B, D: Positive ion mode).
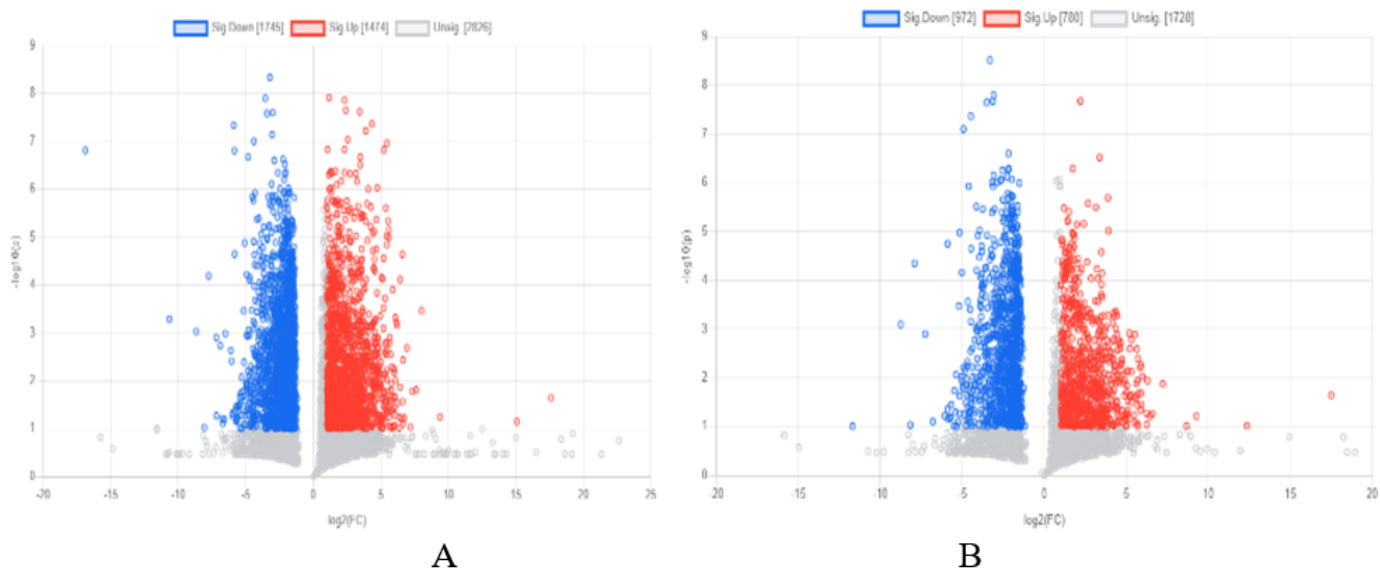
Figure 6

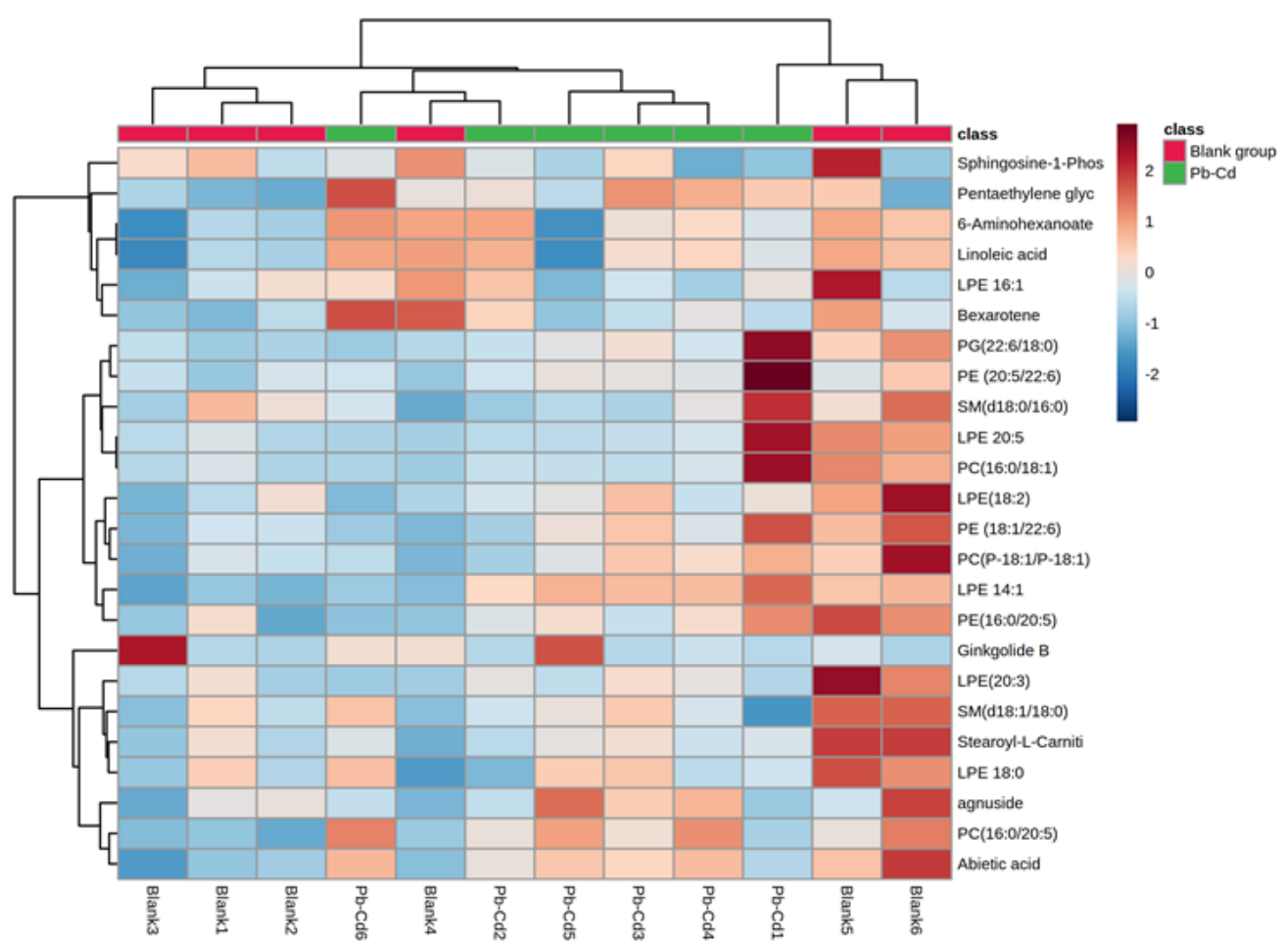Volcano map of differential metabolites (A: Negative ion mode; B: Positive ion mode).

Figure 7

Lipid hierarchical cluster diagram of the tour groups (The red indicated that lipid metabolites were up-regulated, while the green indicated that lipid metabolites were down-regulated).
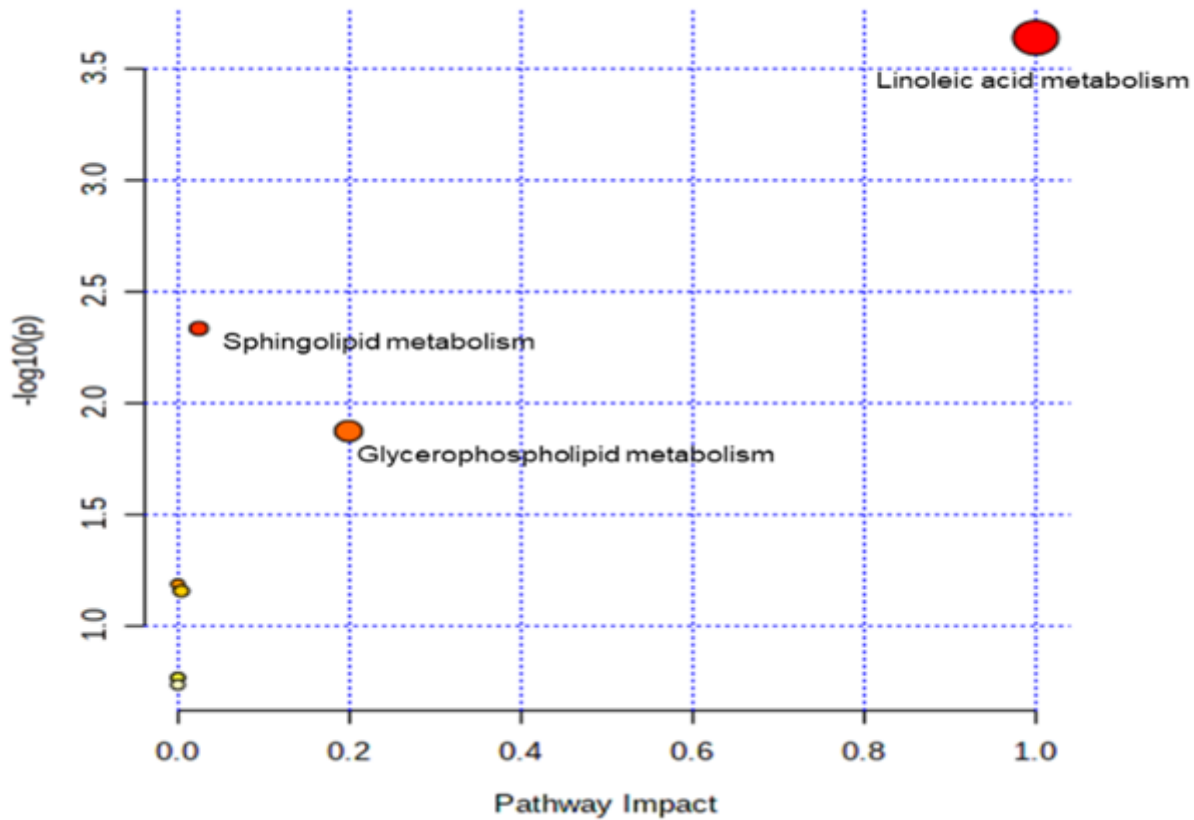

Figure 8

Bubble diagram of differential lipid metabolism pathway.

Supplementary Files

This is a list of supplementary files associated with this preprint. Click to download.

- Supplementaryinformation.doc